

Improved Design of the Axial Flux PM Generator used in Rim Driven Marine Current Turbines

Mohammad Bapiri

dept. of Electrical Engineering
University of Science & Technology
Tehran, Iran

M_bapiri@alumni.iust.ac.ir

Abolfazl Vahedi

dept. of Electrical Engineering
University of Science & Technology
Tehran, Iran

Avahedi@iust.ac.ir

Omid Dorri

dept. of Electrical Engineering
University of Science & Technology
Tehran, Iran

dorri_omid@vu.iust.ac.ir

Abstract— Today, the use of renewable energy, due to its advantages, has become, an integral part of the process of generating electricity in the world. Wind, the sun and seawater flow are the most important renewable energy sources that are used for generating electricity. Marine currents, as part of seawater energy, is an important type of renewable energy, due to its high potential and less impact on environment. The generator used in marine currents is either directly or by gearbox is connected to the turbine. To overcome the problem of maintaining and repairing the gearbox in an area with high-pressure water, the direct drive type is preferred. Another problem in this type of turbine generator, is the interference of the generator in the direction of water flow, because of its location behind the turbine. This problem exists in both gearbox and common direct-drive generators. To overcome this problem, a new kind of direct-drive generator is introduced as Rim-driven. In this type, the rim is located around the turbine blades. Rim-driven structure creates more favorable conditions and has two advantages: first eliminating the problems associated with the gearbox and second not interfering with the flow of water. The rim-driven generators with radial flux and axial flux structures have been studied in several papers. In this paper, the design of an axial flux generator with two rotors is investigated. Since in permanent magnet machines, the weight of magnet affects considerably the final cost of the generator, it is attempted to reduce the weight of magnet and hence the cost of machine compare to similar ones. In fact, by using distributed the same volume of the magnet on the rotor surface, the design is achieved and by applying sensitivity analysis, best geometry that present maximum power is obtained. In the design process, the geometric and magnetic parameters are considered as same as with reference papers in order to provide a better comparison.

software and the accuracy of the results has been investigated and compared.

Keywords— *Direct Drive, Rim Driven, Marine Current, Axial Flux Machine, Renewable Energy*

I. INTRODUCTION

High energy consumption and non-renewable Traditional energy sources, as well as environmental issues, have led governments to use clean energy. [1], illustrates the government's plan to Product a significant amount of energy from renewable energy sources. Marine current energy is one of the most suitable options for renewable power production due to its high potential and predictably.

Marine current energy is to a great extent similar to that of wind turbines, with the difference that in wind turbines, the wind provides Kinetic energy (with high velocity and low density), while in the Marine current energy, water drives the turbine (with very low velocity and high density). This difference makes it possible for a fixed power marine current turbine to have a lower diameter than the wind turbine. Reducing the diameter of the turbine will be very effective in maintaining the environment and the possibility of using more turbines. But the installation of this equipment in areas of the sea and the ocean, which has a

high flow velocity and access to a turbine and generator is difficult, requires high reliability and less maintenance.

given to problems associated with the Marine current and high water flow velocity in the middle of the sea, it is more suitable to use permanent magnet generators due to its high power density and lack of electrical Excitation problems. Another problem that common generators encountered is the maintenance and repairing of generators' gearbox. direct-drive generators can be used for solving this problem. Another problem that can be mentioned here is the disturbance in the flow of water, which causes the movement of water to be slower or disrupted. since we require many generators to generate renewable energy to convert the Kinetic energy into electrical energy, cost minimization of generators can be effective in overall cost savings.

As noted above, using a magnet instead of electric excitation, the eliminating of gearbox and interference in the direction of the water led to the introduction of a new kind of direct-drive generator that called Rim-driven. These kinds of generators use permanent magnets typically. for eliminating the gearbox and interference in the direction of the water, the rotor is placed in the rim around the turbine blades.

Reduction of production cost is an important parameter. the increased diameter of the generator in rim-driven machines, Leads to build rim-driven generators at a lower cost in comparison to the similar power generators. for above reasons, a rim-driven generator is preferred to extract marine energy.

In many references, marine energies have been studied, but reference [2] had investigated designing a rim-driven generator with two stators. In this paper, the design process of the generator has been thoroughly investigated and simulated From the point of view of magnetic and thermal theory, with finite element software. The aim of this paper is to optimize and reduce the cost of the generator structure with the improved design. In this reference, information about the sea flow Turbines of the French La Rance Power Plant is available. (turbines' speed is 15 rpm). The diameter of the turbine is 11 meters and the output power is 300 kW. [3], investigated a rim-driven permanent magnet generator with two rotors and show that the structure cost this type of generator is lower than that of reference [2]. In this paper, the generator didn't optimize.

In this paper, a two-rotor axial flux rim-driven generator is designed. In the first section, the design process is explained. In the next section, a prototype is designed and simulated. after that, considering the fact that the highest cost of the structure is related to the magnet, this paper tried to determine the best structure for properly distributing the volume of the magnet on the rotor by examining the change in the dimensions of the magnet. The purpose of this paper is to reduce the cost of generator structure in comparison with

DSAFPM and RFPM models in [2], DRAFPM model in [3]. At each section, the finite element analysis has been used to validate the results.

II. DIMENSIONAL EQUATIONS

In this section, the complete process of analytical design comes with details:

$$E = \pi k_i N \phi f \quad (1)$$

$$\phi = \frac{(D_o^2 - D_i^2) \pi \alpha B_{mg}}{8 p k_d} \quad (2)$$

$$I = \frac{A_m \pi (D_o + D_i)}{4 m N} \quad (3)$$

$$P_0 = \frac{\pi^3 k_i f A_m \alpha B_{mg} \eta (D_o^2 - D_i^2) (D_o + D_i)}{32 p k_d} \cos(\phi) \quad (4)$$

These design parameters are as follows:

E: Phase RMS Voltage [v]

I: Phase RMS Current [A]

N: Number of Turns per Phase

m: Number of Phases

α : Average constant

B_{mg} : Flux Density in Air Gap [T]

D_o : Outer Diameter [m]

D_i : Inner Diameter [m]

f: Current fundamental frequency [Hz]

k_i : Current waveform factor

P: Pole pairs

k_d : Permanent Magnet Leakage Coefficient

A_m : Electrical Loading $\left[\frac{A}{m} \right]$

η : Efficiency

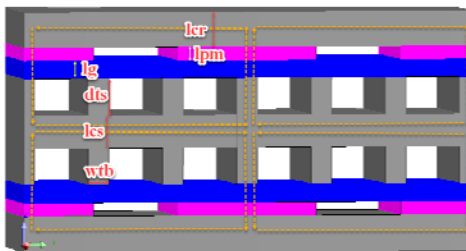


Fig. 1. Dimensions Parameters of Generator Structure

A. Flux relations in different directions of the generator

As shown in Fig.1, the stator flux enters the magnet through the air gap and then enters the yoke of the rotor. The flux is divided into two parts after entering the rotor yoke, in this case. the flux of the stator yoke and the air gap flux are equal.

$$\phi_{(cs)} = \phi_g \quad (5)$$

Since the magnet flux in the rotor yoke is divided into two parts, We will have the following relation:

$$\phi_{(PM)} = 2\phi_{cr} \quad (6)$$

The above relations are in the ideal state, but in reality, due to the leakages Coefficient of the magnet, the relations change as follows:

$$\phi_{(PM)} = \frac{\phi_g}{k_d} \quad (7)$$

$$\phi_{(cs)} = \frac{\phi_g}{k_d} \quad (8)$$

$$\phi_{cr} = \frac{\phi_{(PM)}}{2} \quad (9)$$

$$\phi_g = \frac{\pi(D_o^2 - D_i^2)}{4} \times \frac{1}{2p} \alpha B_{mg} \quad (10)$$

B. The axial length of the rotor yoke

The flux of the rotor yoke is as follows, B_{cr} is the saturation flux density of the rotor core:

$$\phi_{cr} = \frac{(D_o - D_i)}{2} l_{cr} B_{cr} \quad (11)$$

Given the relations (7), (9), (10), (11):

$$l_{cr} = \frac{\pi(D_o + D_i)}{8 p B_{cr}} k_d \alpha B_{mg} \quad (12)$$

C. The axial length of the stator

The flux of the stator core is as follows:

$$\phi_{(cs)} = \frac{(D_o - D_i)}{2} l_{cs} B_{cs} \quad (13)$$

B_{cs} is the saturation flux density of the stator core. The axial length of the stator core is obtained by equating the relations (8) (10) (13):

$$l_{cs} = \frac{\pi(D_o + D_i)}{4 p k_d B_{cs}} \alpha B_{mg} \quad (14)$$

D. The axial length of the magnet

To calculate the axial length of the magnet, [3] has used Ampere's circuital law. If the ohm law is written in one of the loops of figure one, the equation of the Ampere's circuital law will be as follows:

$$2H_{PM}l_{PM} + 2H_g l_g + H_{cs}l_{cs} + H_{cr}l_{cr} = 0 \quad (15)$$

Which is H_{PM} . H_g . H_{cs} . H_{cr} respectively are the intensity of the magnetic field in the magnet, the air gap, the stator core, and the rotor core. It should be taken into account that the intensity of the magnetic field of the rotor and stator core is very small compared to the air gap and magnet. On the other hand, the magnet flux density, if assumed to be linear, is as follows:

$$B_{PM} = B_r + \mu_0 \mu_r H_{PM} \quad (16)$$

As B_r is the residual flux density of the magnet, according to the relations (15) (16), the length of the magnet is obtained as follows:

$$l_{PM} = \frac{\mu_r \alpha B_{mg} l'_g}{B_r - k_d B_{mg}} \quad (17)$$

That l'_g is the effective airgap length.

E. Tooth width

Flux entering the air gap is from through the teeth if N_{spp} is the number of slots per pole, the input flux of the

air gap entered from through these teeth. φ_{ct} is the passing flux from each tooth. we will have the following relations:

$$N_{spp}\varphi_{ct} = \varphi_g \quad (18)$$

$$\varphi_{ct} = B_{ct} \cdot w_{tb} \cdot \frac{(D_o - D_i)}{2} \quad (19)$$

By combining the relations (10) and (19), the width of the tooth is calculated:

$$w_{tb} = \frac{\pi\alpha B_{mg} (D_o + D_i)}{4N_{spp}PB_{ct}} \quad (20)$$

The B_{ct} and w_{tb} are respectively the saturation flux density of tooth and tooth width. The slots width is also obtained by the following relation:

$$w_{sb} = \tau_s - w_{tb} \quad (21)$$

which τ_s is the slot pitch that calculated as follows:

$$\tau_s = \frac{\pi D_i}{Q} \quad (22)$$

And in the above relation, Q is the number of stator slots.

F. Calculate the slots height

To calculate the slots Height, it is necessary to calculate the number of conductors in each slot and diameter of each conductor. According to the relations (1), (2) the number of turn in each phase and the required EMF can be calculated as follows:

$$N = \frac{4EPk_d}{k_i k_w f \pi \alpha B_{mg} (D_o^2 - D_i^2)} \quad (23)$$

If the Wiring have not the parallel path, the radius of each conductor is equal to (j is the current density)

$$r_w = \sqrt{I / (\pi j)} \quad (24)$$

If there is $N_{sl} a$ conductor in each slot and the slots fill factor is equal to k_{cp} , the slot area is obtained:

$$A_{slot} = \frac{\pi r_w^2 N_{sl}}{k_{cp}} \quad (25)$$

By combining relations (21) and (25), the slots height is also calculated.

$$d_{ts} = \frac{A_{slot}}{w_{sb}} \quad (26)$$

G. Calculation of inductance and reactance of machine

In this section, the armature reaction reactance, synchronous reactance, and the stator dispersion reactance are calculated.

a) Armature reaction reactance and synchronous reactance: Synchronous reactance in each phase is expressed by the following equations [4]:

$$X_{sd} = X_{ad} + X_1 \quad (27)$$

$$X_{sq} = X_{aq} + X_1 \quad (28)$$

That X_{sd} , X_{sq} are the machines armature reaction reactances and X_1 is the stator leakage reactance. The machines armature reaction reactances are calculated by the

following relations:

$$X_{ad} = 2m\mu_0 f \left(\frac{N_1 k_{w1}}{p} \right)^2 \frac{(R_o^2 - R_i^2)}{g_d} \quad (29)$$

$$X_{aq} = 2m\mu_0 f \left(\frac{N_1 k_{w1}}{p} \right)^2 \frac{(R_o^2 - R_i^2)}{g_q} \quad (30)$$

$$g'_d = g'_q = g' = g_e + \frac{l_{PM}}{\mu_r} \quad (31)$$

b) Stator dispersion reactance: armature dispersion reactance obtained from the total slot dispersion reactance X_{ls} , End connection Distribution reactance X_{le} and Differential dispersion reactance X_{ld} [4]:

$$X_1 = X_{ls} + X_{le} + X_{ld} = 4\pi f \mu_0 \frac{L_i N_1^2}{pq_1} (\lambda_{ls} + \lambda_{le} + \lambda_{ld}) \quad (32)$$

The values of λ_{ls} , λ_{le} , λ_{ld} are Calculated in the following.

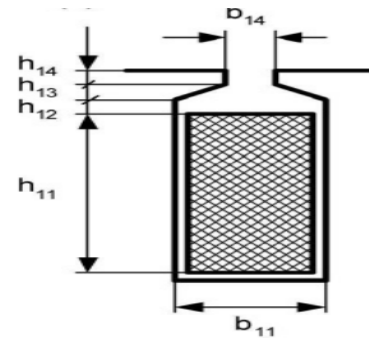


Fig. 2. Half open Rectangular slot

The slots dispersion permeance coefficient λ_{ls} is calculated for the different shapes of the slot as follows [4]:

$$\lambda_{ls} = \frac{h_{11}}{3b_{11}} + \frac{h_{12}}{b_{11}} + \frac{2h_{13}}{b_{11} + b_{14}} + \frac{h_{14}}{b_{14}} \quad (33)$$

The End connection permeance λ_{le} is estimated on the basis of experience and is calculated approximately from the following equation:

$$\lambda_{le} \approx 0.2q_1 \quad (34)$$

The Differential dispersion flux permeance λ_{ld} is calculated from the following equation:

$$\lambda_{ld} = \frac{mq_1 \tau k_{w1}}{\pi^2 g} \tau_{d1} \quad (35)$$

Which τ is the pole-pitch and τ_{d1} is calculated from the following equation:

$$\tau_{d1} = \frac{\pi^2 (10q_1^2 + 2)}{27} \left[\sin\left(\frac{30}{q_1}\right) \right]^2 - 1 \quad (36)$$

H. Calculate the mains and leakage fluxes' permeance

According to [5], the components of the permeance are

calculated as follows:

$$G_{g1} = \mu_0 \frac{\pi \alpha_i (D_o^2 - D_i^2)}{8 p g} \quad (37)$$

$$G_{g2} = 0.52 \mu_0 \frac{D_o - D_i}{2} \quad (38)$$

$$G_{g3} = \frac{3.26 \alpha_i}{2 p} \mu_0 \left(\frac{D_i}{2} + \frac{g}{4} \right) \quad (39)$$

$$G_{g4} = \frac{3.26 \alpha_i}{2 p} \mu_0 \left(\frac{D_o}{2} + \frac{g}{4} \right) \quad (40)$$

$$G_{g5} = \frac{2 \alpha_i}{2 p} \mu_0 (D_i + g) \ln \left(1 + \frac{l_{PM}}{g} \right) \quad (41)$$

$$G_{g6} = \frac{2 \alpha_i}{2 p} \mu_0 (D_o + g) \ln \left(1 + \frac{l_{PM}}{g} \right) \quad (42)$$

$$G_{g7} = \mu_0 \frac{2(D_o - D_i)}{2 \pi} \ln \left(1 + \frac{l_{PM}}{2g} \right) \quad (43)$$

$$G_{g8} = 0.308 \mu_0 g \quad (44)$$

$$G_{g9} = \mu_0 \frac{l_{PM}}{4} \quad (45)$$

Airgap permeance is calculated as follows [5]:

$$G_g = G_{g1} + 2(G_{g2} + G_{g7}) + G_{g3} + G_{g4} \quad (46)$$

$$+ G_{g5} + 4(G_{g8} + G_{g9})$$

The components of leakage flux permeance are also calculated as follows [5]:

$$G_{g10} = \frac{3.26 \alpha_i}{2 p} \mu_0 \left(\frac{D_i}{2} + \frac{l_{PM}}{8} \right) \quad (47)$$

$$G_{g11} = \frac{3.26 \alpha_i}{2 p} \mu_0 \left(\frac{D_o}{2} + \frac{l_{PM}}{8} \right) \quad (48)$$

$$G_{g12} = 0.52 \mu_0 \left(\frac{D_o - D_i}{2} \right) \quad (49)$$

$$G_{g13} = 0.308 \mu_0 \frac{l_{pm}}{2} \quad (50)$$

leakage flux permeance is calculated as follows:

$$G_{PM} = G_{g10} + G_{g11} + 2G_{g12} + 4G_{g13} \quad (51)$$

Magnets leakage flux coefficient is calculated as follows:

$$k_d = 1 + \frac{G_{PM}}{G_g} \quad (52)$$

The magnets permeance is calculated as follows:

$$G_m = \frac{\alpha_i \pi \mu_r \mu_0}{8 p l_{PM}} (D_o^2 - D_i^2) \quad (53)$$

The maximum flux density is calculated as follows:

$$B_{mg} = \frac{G_g}{2G_{PM} + G_m + G_g} B_r \quad (54)$$

III. PROTOTYPE DESIGN RESULTS

Table 1 shows the design specification of the generator.

TABLE I. MCT¹ DESIGN SPECIFICATION

	Definition	Value	Unit
P _m	Mechanical power	300	kW
w _r	Turbine speed	15	rpm
R _i	Rotor inner radius	5.5	m
T	Torque	191	kNm
p	Number of pole pair	200	-
N _{ph}	Number of phases	3	-
H _c	Magnet coercive field	-10 ⁶	A/m
B _{mg}	Maximum air gap flux density	0.6	T
B _r	Magnet residual flux density	1.22	T
B _{cr,cs,ts}	Maximum magnet flux density in the stator yoke iron, rotor yoke iron, and teeth iron	1.4	T
k _{cp}	Slot fill factor	0.65	-
A _m	Electrical loading	80000	A/m
J _m	Copper current density	7.15	A / mm ²

Considering the specifications used in [3] and mentioned relations in the previous section, the generator's design was performed and simulated with the Flux software. Due to the fact that the flux leakage of the magnet reduces flux in the air gap than what is expected of the design, a loop is used to try and error so that the flux in relation to the magnet length, the height of the stator core and the rotor, and... equal to that calculated in equation (54) for that the difference between the analytical results and the finite element is minimized.

Simulations are performed in full load and in no load. At full load, the electromagnetic power of the generator is calculated. According to reference [5], the iron losses are 3% of rated power, which is 9 kW in this case. On the other hand, the input power is equal to the sum of iron losses and electromagnetic power. In this way, the electromagnetic power is 291kW and iron losses are 9kW, so the input power of the generator is 300kW. Using the relations in Section 2, the geometric parameters of the machine are calculated in Table 2.

TABLE II. DESIGN PARAMETERS

	Definition	Value	Unit
D _o	Outer Diameter	11.128	m
D _i	Inner Diameter	11.030	m
l _{cr}	Rotor Yoke Length	12.6	mm
l _{cs}	Stator Yoke Length	17.43	mm
l _{pm}	PM length	4.736	mm
d _{ts}	Slot depth	13.22	mm
w _{tb}	Tooth width	9.97	mm

¹ Marine Current Turbine

In Table 3, the simulation results are compared with the analytical calculations. Table 3 shows that there is little difference between an analytic relation and finite element. In this generator, 9 kW is wasted in the iron losses section. The copper losses are 30.5 kW and the generator Efficiency at full load is 87%. According to [3], the cost per kilogram of iron is 0.67 \$, one kilogram of copper is 8\$, and per kilogram of NdFeB magnet is 115.7\$. Table 4 shows that the total cost of this generator is 12500 \$.

TABLE III. RESULTS OF THE FINITE ELEMENT AND ANALYTICAL DESIGN

	Definition	Analytical	FEA	Unit
P_m	Mechanical power	299	299.67	kW
E	Fundamental phase back-EMF(rms)	304	307	V
I_{ph}	Current(rms)	387	390	A
X_s	Reactance	0.447	0.42	Ω
R_s	Winding Resistor	0.062	0.062	Ω
B_{cr}	Rotor yoke peak flux density	1.4	1.4	T
B_{cs}	Stator yoke peak flux density	1.4	1.4	T
B_g	Air gap peak flux density	0.481	0.51	T

TABLE IV. WEIGHT AND COST OF THE GENERATOR

Definition	Value	Unit
P_{in}	299.67	W
P_{out}	260.2	W
Efficiency	87	%
PM Weight	84	kg
Cooper Weight	292	kg
Stator & Rotor Weight	679	kg
Total Weight	1055	kg
PM Price	9718	\$
Cooper Price	2336	\$
Stator & Rotor Price	454	\$
Total Price	12508	\$

Figure 3 shows the distribution of the flux density in the stator and rotor core. The simulation shows the maximum flux density in the core is less than 1.4 Tesla. Figure 4 shows the flux density at a cross-section of the air gap over a period of time. The maximum flux density at this point is 0.51 Tesla, which was calculated 0.481 Tesla in the analytical section.

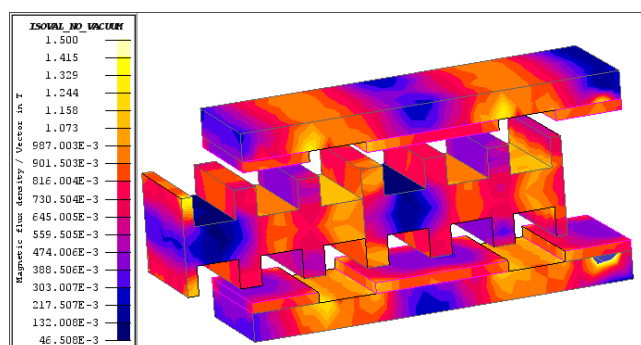


Fig. 3. Distribution of stator core and rotor flux density

To calculate the EMF, the simulation has been done at no load. Figure 5 shows the EMF waveform generated by simulation and analytical calculations. In this figure, the EMF value of simulation is 307 volts, which is only 1 volt different compared to 308 volts in the analytical calculations.

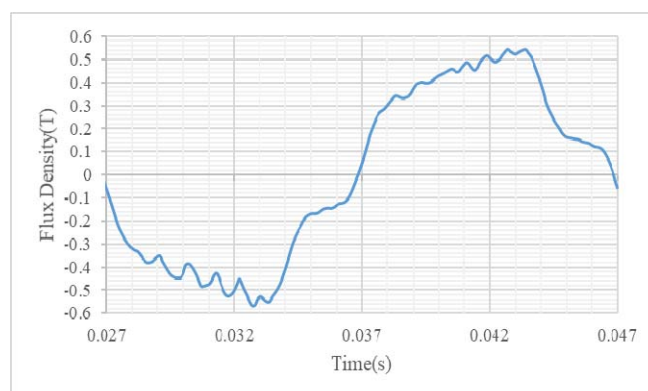


Fig. 4. Airgap flux density over a period of time

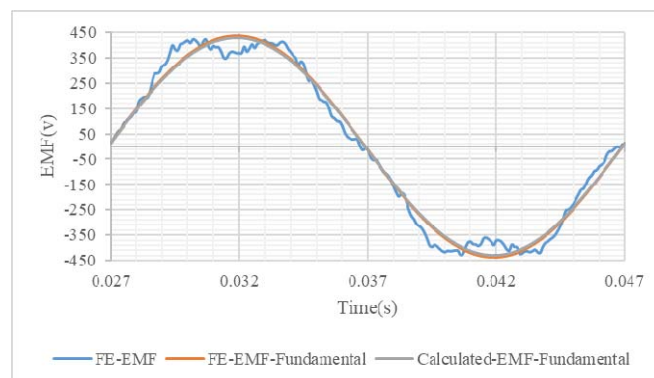


Fig. 5. Comparison of analytical and finite element EMF Waveform

IV. SENSITIVITY ANALYSIS

This section shows what kind of distribution for magnets on the rotor can produce more electromagnetic power. Magnet volume is constant and equal to that calculated in the previous section. Except for the four cases, the height of the magnet, the depth of the stator and the rotor core, and the external diameter of the generator, all the geometric parameters are considered constant. The magnet volume increases with increasing outer diameter. The change in the height of the magnet causes it to stay constant. On the other hand, the change in the depth of the stator and the rotor core is proportional to the change in the outer diameter, causes the flux density to remain constant. By changing the outer diameter, the intensity of the magnet volume distribution in axial or radial direction with a constant ratio of pole-shoe wide to pole-pitch has been investigated. Fig. 3 and Fig. 4, respectively, show the electromagnetic power variation and the average electromagnetic power for each external diameter.

It can be clearly seen in Fig. 7 that by increasing the outer diameter and reducing the axial length of the magnet to a certain extent, more electromagnetic power can be obtained from the machine. According to the above results, now the design results of section I have been modified with the aim of reducing the weight of the magnet and producing

300 kW power. Figure 7 shows that the maximum power is obtained in $D_o = 11.150\text{m}$.

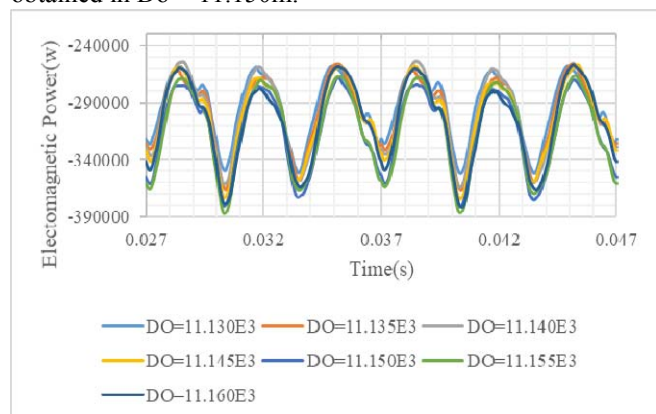


Fig. 6. Generator Electromagnetic Power in Different Do

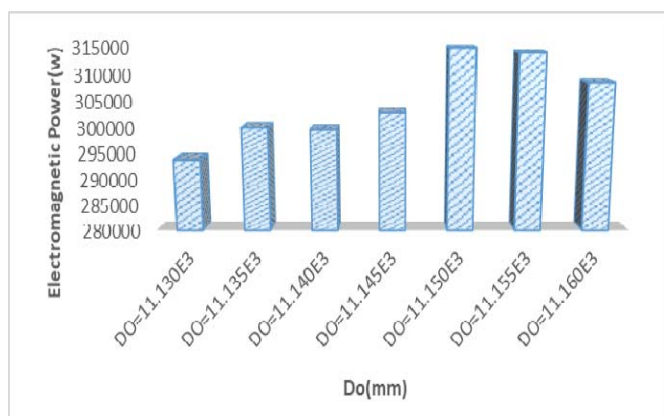


Fig. 7. Average of Generator Electromagnetic Power in Different Do

V. IMPROVED DESIGN

According to the results of the sensitivity analysis, it has been found that by increasing the outer diameter, more electromagnetic power can be obtained in a constant volume of the magnet. In order to maintain an electromagnetic power in 291 kW constant with 11.150 mm diameter, it should be reduced the dimensions related to the height of the magnet and the depth of the stator and the rotor core. Table 5 shows the modified geometry parameters of the generator. Table 6 and Figure 10 show the power input, EMF, and rated current of the improved generator, which EMF has increased 17 volts compared to the previous design.

Table 7 lists the cost and weight of the generator. By comparing Table 7 and Table 4, it is clear that the cost of construct the generator has reduced from 12508\$ to 12159\$.

TABLE V. IMPROVED DESIGN PARAMETERS

	Definition	Value	Unit
D_o	Outer Diameter	11.150	m
D_i	Inner Diameter	11.030	m
l_{cr}	Rotor Yoke Length	9.3	mm
l_{cs}	Stator Yoke Length	12.9	mm
l_{pm}	PM length	3.676	mm
d_{ts}	Slot depth	13.22	mm
w_{tb}	Tooth width	9.97	mm

TABLE VI. IMPROVED DESIGN ELECTRICAL OUTPUT RESULTS

	Definition	FEA	Unit
P_m	Mechanical power	299.85	kW
E	Fundamental phase back-EMF(rms)	324	V
I_{ph}	Current(rms)	386.1	A

TABLE VII. COST AND WEIGHT OF THE IMPROVED DESIGN

Definition	Value	Unit
P_{in}	299.85	W
P_{out}	257.1	W
Efficiency	86	%
PM Weight	79.6	kg
Cooper Weight	314	kg
Stator & Rotor Weight	654	kg
Total Weight	1047.6	kg
PM Price	9209	\$
Cooper Price	2512	\$
Stator & Rotor Price	438	\$
Total Price	12159	\$

Figure 8 shows the distribution of the flux density in the core of the generator, which displays the density of the flux is less than 1.4. Also, the full load results show that the air gap flux density, as shown in Fig. 9, has reduced to 0.481.

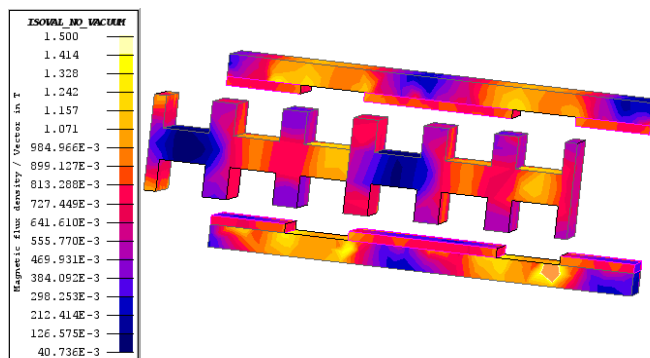


Fig. 8. Distribution of flux density in the rotor and stator core of the improved design

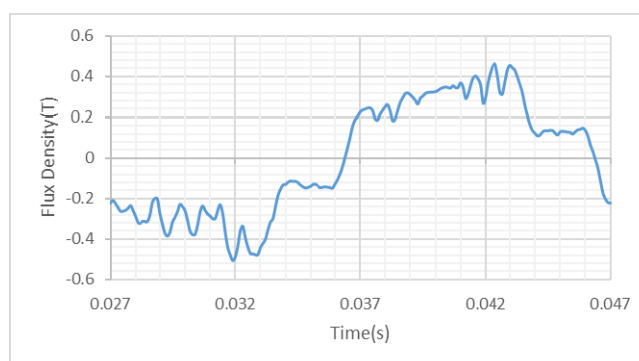


Fig. 9. Airgap flux density in improved design over a period of time

After initial design and sensitivity analysis, the generator was designed to reduce costs. As mentioned in the introduction section, several papers have been published to design a generator of the same dimensions. Figure 11 shows that the generator introduced in [3] has a lower active part weight than other generators, but since the highest cost is related to the magnets, the improved generator has lower magnet weight than the generator introduced in [3]. Therefore,

according to Fig. 12 it can be seen that the improved generator in this section has less cost-effective than all other similar generators.

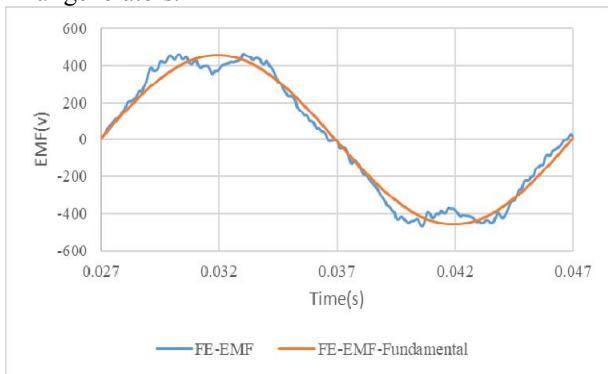


Fig. 10. EMF waveform in improved design

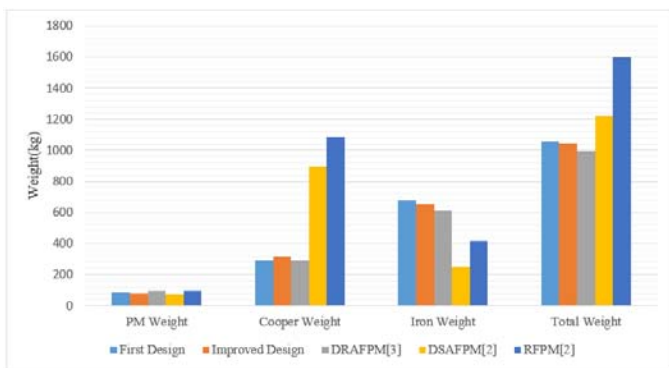


Fig. 11. Compare the weight of active parts

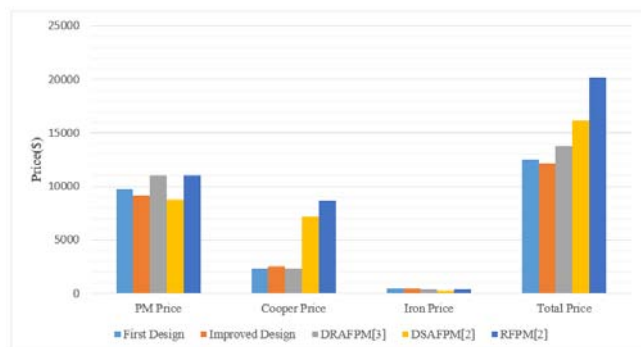


Fig. 12. Compare the cost of active parts

VI. CONCLUSION

This paper presents the structure of AFPM-NN generator at a lower cost than the similar ones, for converting the energy of a marine current turbine. In this research to increase the accuracy of the analytical calculations, the effect of modified flux density and the leakage flux in the air gap have been calculated. An analytical electrical design was carried out in the first section and geometric characteristics of the machine were calculated. The analytical calculations results were verified by finite element method. The power and EMF results of the analytical calculations were very close to the finite element method results. The designed generator with Efficiency 87% had cost 12508\$, which had the lower cost than the similar generators. By modifying the magnet dimensions by sensitivity analysis, the generator cost has reduced to 12159\$. This reduction in the cost will be very significant for power plants because a large number of marine current turbines will be used.

REFERENCES

- [1] P. Donohoo-Vallett, "The Future Arrives for Five Clean Energy," U.S. Department of Energy (DOE), 2016.
- [2] Djebbari, Sofiane; Charpentier, Jean Frédéric; Sculler, Franck; Benbouzid, Mohamed, "Design and Performance Analysis of Double Stator Axial Flux PM Generator for Rim Driven Marine Current Turbines," *IEEE Journal of Oceanic Engineering*, vol. 41, no. 1, pp. 50 - 66, 2016.
- [3] Kim, Ju Hyung; Sarlioglu, Bulent, "Preliminary design of axial flux permanent magnet machine for the marine current turbine," in *IECON 2013 - 39th Annual Conference of the IEEE Industrial Electronics Society*, Vienna, Austria, 2013.
- [4] Jacek, F; Gieras, Rong; Wang, Jie; Kamper, Maarten J, *Axial Flux Permanent Magnet*, 2 ed., New York: Kluwer Academic, 2008.
- [5] T. D. Nguyen, "Dual Air-Gap Axial Flux Permanent Magnet Machines for Flywheel Energy Storage Systems," Centre for Smart Energy Systems, 2012.
- [6] A. M. EL-Refaie, "High-speed operation of permanent magnet machines," University of Wisconsin-Madison, 2005.